

Au@Ag core-shell Nanomaterials Embedded in N-doped graphene: A Novel Electrochemical Sensor for Determination of Gallic Acid

Shaoping Feng^{1,2,3}, Xinghuai Zhou^{1,2}, Xianlan Chen^{1,2,*}, Guowei Zhang^{1,2,*}, Guiyang Liu^{1,2,*}, Na Wu^{1,2}, Wei Liu^{1,2}

¹ College of Science, Honghe University, Mengzi, 661199, Yunnan, P.R.China

² Local Characteristic Resource Utilization and New Materials Key Laboratory of Universities in Yunnan, Honghe University, Mengzi, 661199, Yunnan, China

³ School of Metallurgical and Ecological Engineering, University of Science and Technology Beijing, Beijing 100083, China

*E-mail: 13489086418@163.com, yunnmzh@126.com, alios@126.com

Received: 28 February 2020 / Accepted: 19 April 2020 / Published: 10 June 2020

A hydrothermal method was employed to synthesize N-doped graphene (NG) with graphenes oxide (GO) as raw material, urea ($\text{CH}_4\text{N}_2\text{O}$) as nitrogen source and reductant. Nitrogen atoms have successfully bonded with carbon atoms of graphene with the high relative atomic ratio (7.34 %). Then, the NG was impregnated with Au@Ag core-shell nanoparticles (Au@Ag NPs) which prepared by seed-mediated growth method to synthesize N-doped Au@Ag core-shell nanoparticles (NG-Au@Ag NPs). The NG-Au@Ag NPs present wrinkled sheets on the surface and maintain a similar spherical morphology, and were composed of Au, Ag and NG elements. After that, the NG-Au@Ag NPs were dropped on glassy carbon electrode (GCE) for sensing gallic acid (GA). Under the optimal experimental procedure, the electrochemical sensor for GA exhibited a good linear range of 1.0×10^{-6} - 1.62×10^{-5} M and the detection limits was 3.17×10^{-9} M (S/N=3). The proposed electrochemical sensor was used to determination of GA in black tea samples with satisfactory recovery range (96.12-100.50%) and relative standard deviation (RSD, 1.52-2.03%), indicating its feasibility for GA determination.

Keywords: N-doped graphene; Au@Ag NPs; Gallic acid; Electrochemical sensor

1. INTRODUCTION

Gallic acid (GA, 3,4,5-trihydroxybenzoic acid) was an organic acid existing in several plants such as grapes, witch hazel, gallnuts, especially in green and black teas [1]. GA has been usually used in pharmaceutical and food industries due to its free radical scavenging properties [2]. More

significantly, the results of clinical research show that GA and its derivatives also possess biological properties including anti-cancer, antihistaminic, antimutagenic and anti-inflammatory [3]. Due to its biological activities, GA exhibits potential applications in clinical medicine and has received considerable attention. Therefore, developing an efficient and sensitive method for determination of GA concentration in real samples is essential for illuminating and developing pharmacological research.

In past years, various analytical procedures for determination of GA have been applied, such as HPLC [4-6], ultra-performance liquid chromatographic method (UPLC) [7], TLC [8], LC-ESI/MS [9] and electrochemical detection [10, 11]. It is the electrochemical analysis that has recently attracted much attention as it exhibits certain advantages, such as high sensitivity, low-cost and wide dynamic range [1, 12]. J. Tashkhourian reported a SiO₂ nanoparticle modified carbon paste electrode (SiO₂ nanoparticle-CPE) and used as a sensor for detection of GA in teas and orange juice samples with a low detection limit (2.5×10^{-7} M) [1]. Liang successfully constructed a AuMCs/SF-GR/GCE sensor and successfully applied to determinate GA and uric acid (UA) in urine samples [3]. Luo constructed the polyethyleneimine-functionalized graphene oxide modified glassy carbon electrode (PEI-rGO/GCE) and successfully applied to determination of GA in green and black tea samples [12]. Refat Abdel-Hamid reported a glassy carbon electrode modified with polyepinephrine (PEP/GCE) for detection of GA in black tea, with the detection limit of 6.63×10^{-7} M [13].

In order to develop an efficient and sensitive method for rapid determination of GA in real samples, the preparation and application of N-doped graphene/Au@Ag core-shell nanomaterials modified electrodes (NG-Au@Ag NPs/GCE) as an electrochemical sensor for determination of GA were proposed. The NG-Au@Ag NPs/GCE was successfully applied to determination of GA in black tea samples with excellent stability and high accuracy.

2. EXPERIMENT

2.1 Reagents

HAuCl₄, AgNO₃, ascorbic acid (C₆H₈O₆) and urea (CH₄N₂O) were purchased from Sinopharm Chemical Reagent Co. Ltd. (Shanghai, China). Graphite powder (99.95%, 325 mesh) was purchased from Alfa Aesar Co. Ltd. (Tianjin, China). The desired working solutions were obtained by diluting the stock solution with ultra-pure water and phosphate buffer solution (PBS, NaH₂PO₄-Na₂HPO₄). All the other chemicals were of AR grade and used without further purification.

2.2 Instruments and characterizations

UV-vis spectra (Perkin-Elmer Lambda 900 USA) was used to obtain UV-vis absorption spectra of Au and Au@Ag NPs. X-ray diffraction (XRD, X'pert, Philips, Holland) was used to ascertain the phase structures of the materials. XPS (Thermal Scientific K-Alpha XPS spectrometer) was employed to investigate the atomic composition ratio of the samples. SEM (Nova Nano SEM 230, FEI, USA)

and HRTEM (Tecnai G2 F20 S-TWIN, 200 kV, FEI Company, USA) were used to obtain the surface morphologies and microstructure of the materials.

Cyclic voltammetry (CV) was performed on electrochemical workstation (CHI 660C, Shanghai). The electrochemical cell consisted of a three electrode system with a bare glassy carbon electrode (GCE, 3.0 mm in diameter) or modified working electrode as a working electrode, a platinum wire as a counter electrode and Ag/AgCl electrode as a reference electrode. PBS (0.20 M, pH= 2.0) was added into the electrochemical cell and all the detection solutions were purged with N₂ for at least 15.0 min before measurements. All measurements were performed at room temperature (25 °C).

2.3 Preparation of Au@Ag NPs

Firstly, Au seeds were synthesized according to Frens' method [14]. Then, 680 µL 1.0 mM AgNO₃ and 320 µL ultra-pure water was dropped gradually into a conical beaker contained 2 mL Au seeds. The mixtures were cooled down to ca. 4.0 °C in an ice bath and stirred for 5.0 min. Finally, 330 µL 10.00 mM ascorbic acid (C₆H₈O₆) was added gradually into the solution and stirred for another 30.0 min. The color of the deep wine solution changed to light yellow, suggesting that the Au@Ag NPs formed. The UV-vis spectra, XRD and TEM of Au@Ag NPs were shown in Fig. 1.

2.4 Preparation of NG and NG-Au@Ag NPs

In this experiment, GO was synthesized by Hummers method [15]. NG was synthesized by a hydrothermal method with GO as raw material, urea (CH₄N₂O) as nitrogen source and reductant. GO and urea (mass ratio of 1:30) were transferred to a magnetic agitated autoclave and heated to 160 °C for 3h to synthesize NG. The TEM, XRD and XPS of NG were shown in Fig. 2 and Fig. 3, respectively. Finally, Au@Ag NPs (1.0 mL) and NG (0.5 mL) were mixed under sonication (200 W) for 3 h until to obtain NG-Au@Ag NPs with uniform dispersion. The TEM and XRD of NG-Au@Ag NPs were shown in Fig. 4.

2.5 Preparation of electrode and analytical procedure

The bare glassy carbon electrode (GCE) was polished with alumina powders (1.0, 0.3 and 0.05 µm) in series. Then, the electrode was ultrasonicated in 1.0 M nitric acid, ethanol and water successively about 5 min after each polishing, respectively. The electrode was dried under pure N₂. Then, 10.0 µL the NG-Au@Ag NPs was uniformly dropped on GCE surface, and a film coated electrode of NG-Au@Ag NPs/GCE was obtained after drying with infrared lamp. Similarly, the NG/GCE and Au@Ag NPs/GCE as compared were fabricated. The modified electrode was renewed after each measurement by a multi-circle potential scan in the potential range (0.0-0.8 V) in a blank PBS (pH= 2.0) until the background CV curve was invariable.

3. RESULTS AND DISCUSSION

3.1 Characterization of Au@Ag NPs

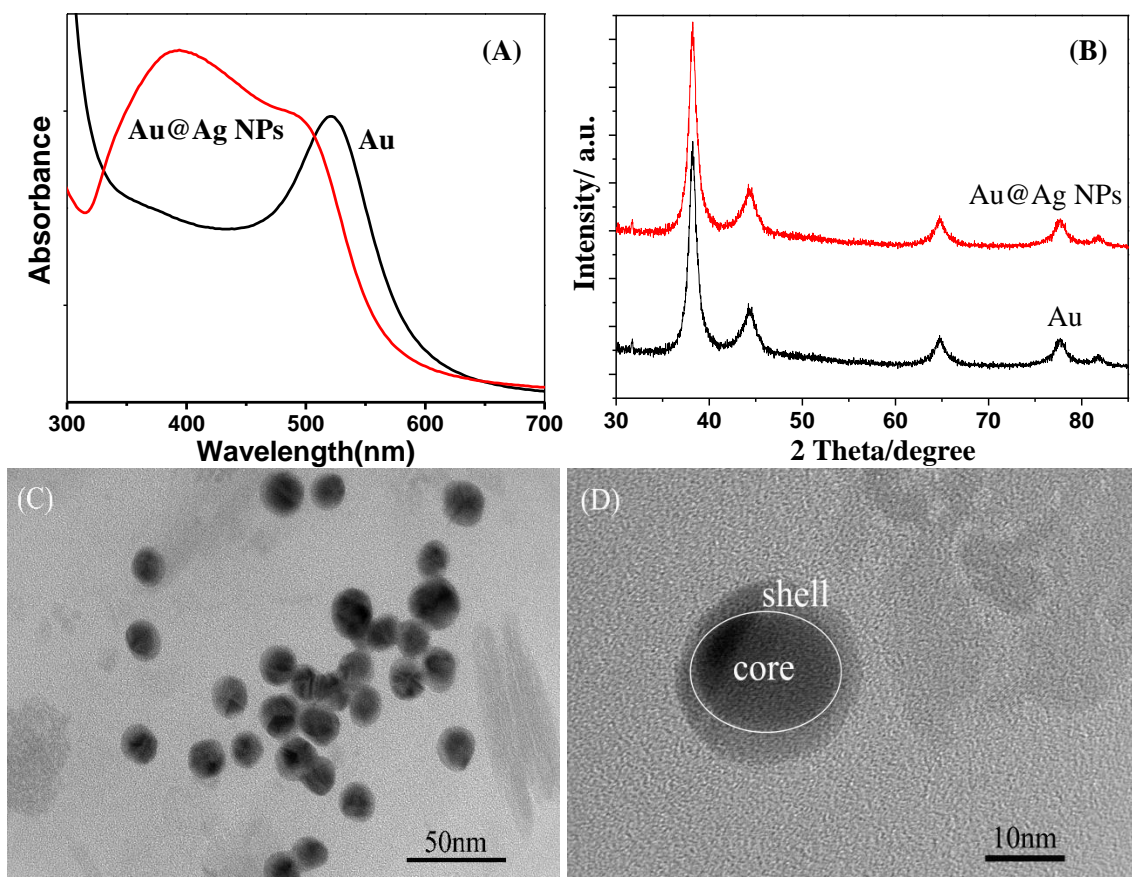


Figure 1. UV-vis spectra of Au and Au@Ag NPs (A). XRD of Au and Au@Ag NPs (B). TEM of Au@Ag NPs at different magnification (C and D)

UV-vis spectra of Au and Au@Ag NPs was shown in Fig. 1(A), the typical absorption peak at 520 nm can be attributed to Au seeds. A new wide absorption peak of Au@Ag NPs appeared at 420 nm belonged to Ag, meaning that Au core was coated with Ag shell. The results indicated that Au@Ag NPs has been successfully synthesized. The XRD of Au and Au@Ag NPs was shown in Fig. 1(B). The diffraction angles (2θ) values of 38.24° , 44.14° , 64.82° and 77.22° result from Au diffractions (Au sample), while the (2θ) values of Au@Ag NPs appeared at 38.16° , 44.14° , 64.74° and 77.34° due to the thinner shell of Au@Ag alloy on Au surfaces [16, 17]. TEM images of resultant Au@Ag NPs were displayed in Fig. 1(C) and (D). It can be founded that Au@Ag NPs were almost uniform spherical morphology with an average diameter of ~ 18.0 nm and consisted of Au cores (~ 15.0 nm) and Ag shells (~ 3.0 nm) growing on Au cores. Therefore, Au@Ag core-shell nanomaterials have been successfully synthesized according to “seeded growth” method [18].

3.2 Characterization of N-doped graphene (NG)

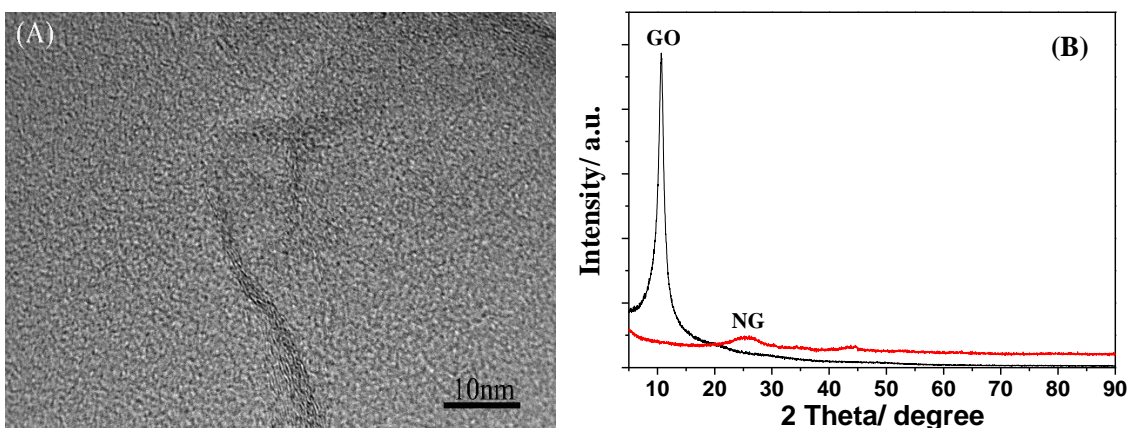


Figure 2. TEM image (A) and XRD (B) of NG

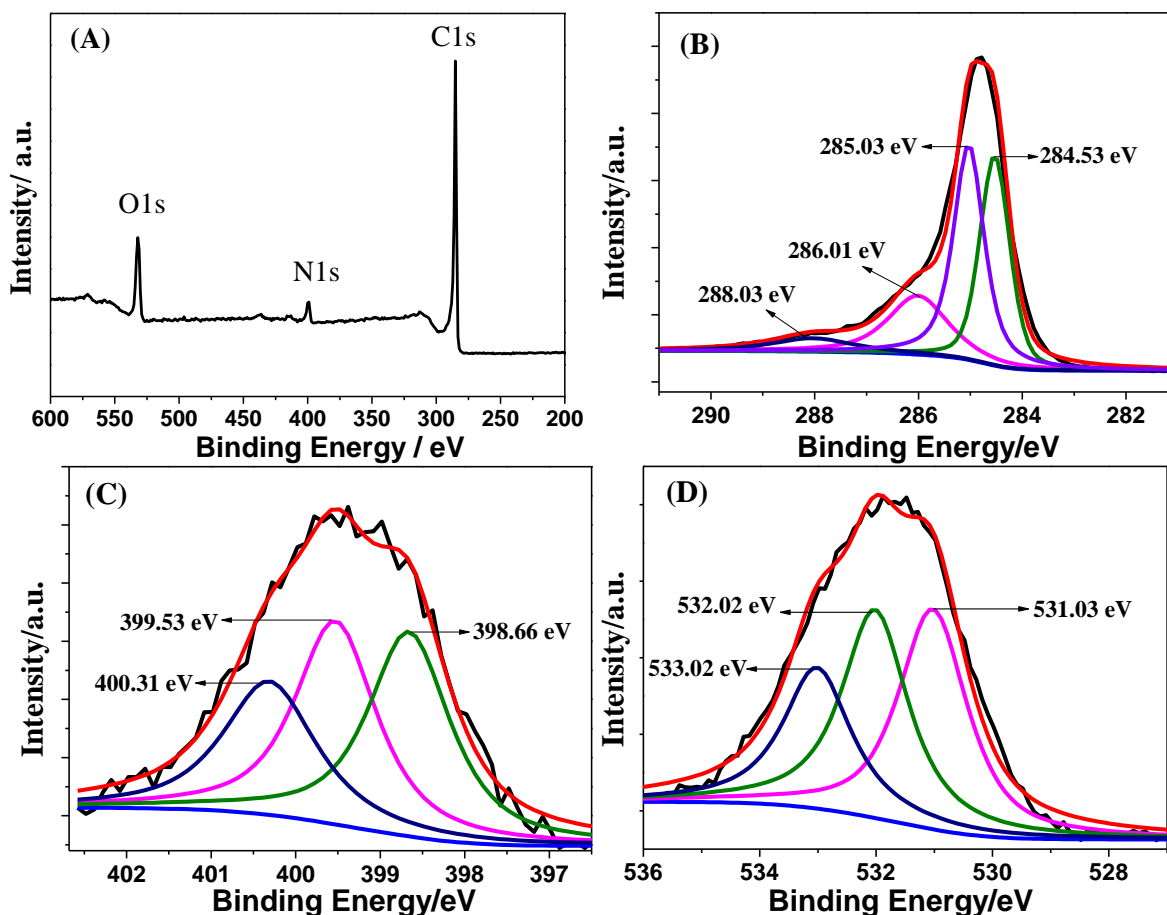


Figure 3. (A) XPS survey spectrum of NG. (B-D) XPS spectrum of C1s, N1s and O1s XPS scan of NG

The morphology of NG was revealed by the TEM images, as shown in Fig. 2(A). A transparent, disorderly and wrinkled sheet of NG was observed. XRD of NG was obtained to

investigate the phase composition, as shown in Fig. 2(B). The 2θ values of 10.68° and 21.68° were responded to GO and NG, respectively. That is to say, a new diffraction peak located at $2\theta = 21.68^\circ$ was observed after N doping, indicating NG was successfully synthesized.

To confirm the element components and the nature of the binding of NG, XPS was employed and the results were shown in Fig. 3. The three distinguishable peaks of C1s (284.81 eV), N1s (399.34 eV) and O1s (531.74 eV) (Fig. 3(A)) suggested that nitrogen atoms have successfully bonded with carbon atoms of graphene. And the relative atomic ratio of C, N, and O were 84.73 %, 7.34 %, and 7.93 %, respectively. This indicated that N doping process using urea through hydrothermal method was effective. Fig. 3(B) showed four fitting peaks of 284.53 eV (C=C), 285.03 eV (C-C/C-N), 286.01 eV (C-O) and 288.03 eV (-COOH) [19]. XPS spectra of N1s was shown in Fig. 3(C), there were three peaks at 398.66 eV (pyridinic N), 399.53 eV (pyrrolic N) and 400.31 eV (graphitic N), meaning three types of species of nitrogen [19]. Three distinguishable peaks with binding energies of 531.03 eV, 532.02 eV and 533.02 eV were corresponded to C=O-OH, C-O and C-OH, respectively [20].

3.3 Characterization of NG-Au@Ag NPs

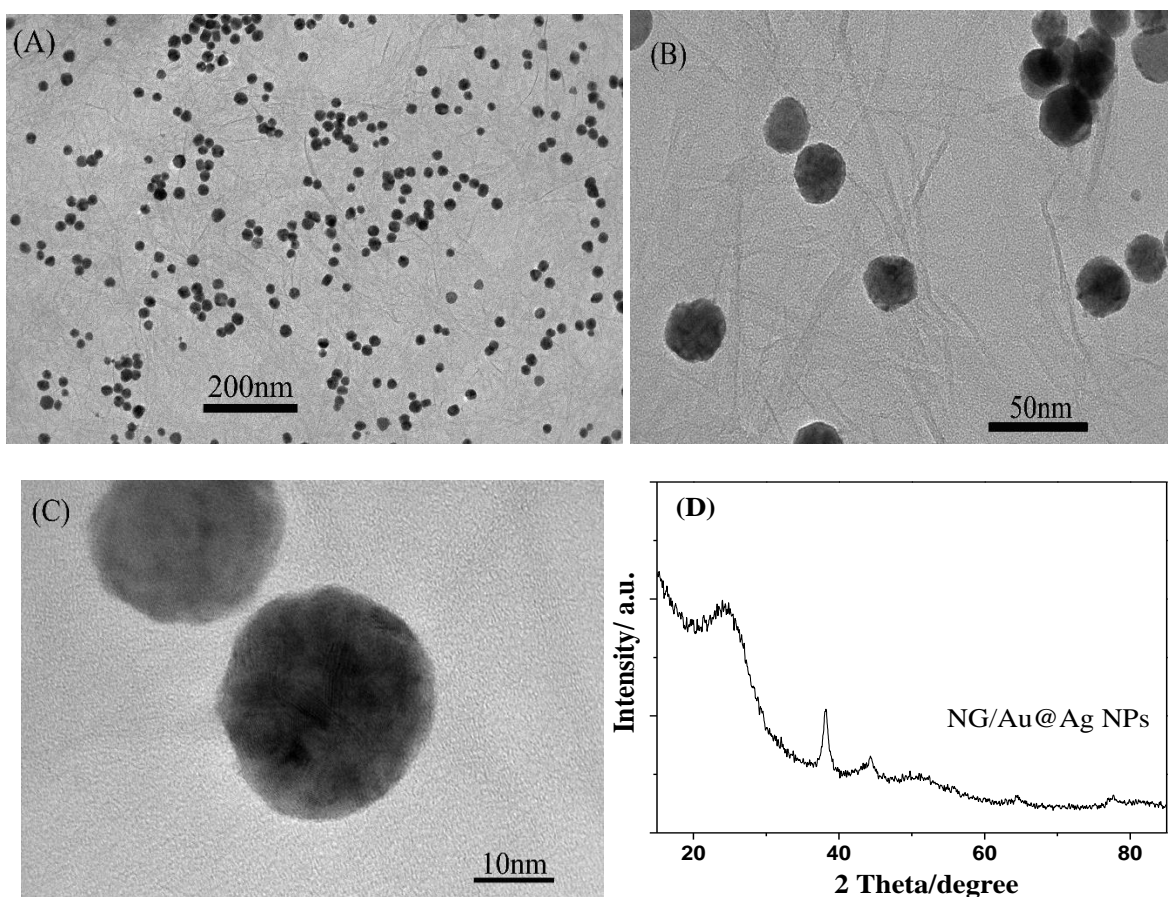


Figure 4. TEM images of NG-Au@Ag NPs at different magnification (A, B and C). (D) XRD patterns of NG-Au@Ag NPs

The structure and morphology of NG-Au@Ag NPs were totally revealed by the TEM images at different magnification in Fig. 4. The numerous Au@Ag NPs were uniformly dispersed the highly transparent NG supports and no obvious aggregation observed (Fig. 4(A)), indicating that Au@Ag NPs can totally anchor on the surface of NG. Moreover, Au@Ag NPs with similar spherical morphology (an average diameter of ~ 23.0 nm) were found on the surface of NG and formed the nanomaterials of NG-Au@Ag NPs (Fig. 4(B) and 4(C)), which still maintain wrinkled sheets. XRD of NG-Au@Ag NPs was obtained to investigate the phase composition and the result was shown in Fig. 4(D). The typical diffraction peak located at $2\theta = 21.42^\circ$ was attributed to the graphene sheets of the (002) plane [21]. The 2θ values of 38.20° , 44.30° , 64.56° and 81.14° were originated from the diffraction peaks of (111), (200), (220) and (311) crystal faces of NG-Au@Ag NPs, respectively, corresponding to the phases of both Au and Ag diffractions [22, 23]. It concludes that NG-Au@Ag NPs was composed of numerous elements including Au, Ag and NG.

3.4 Electrochemical Characterization

3.4.1 Electrochemical behavior of GA

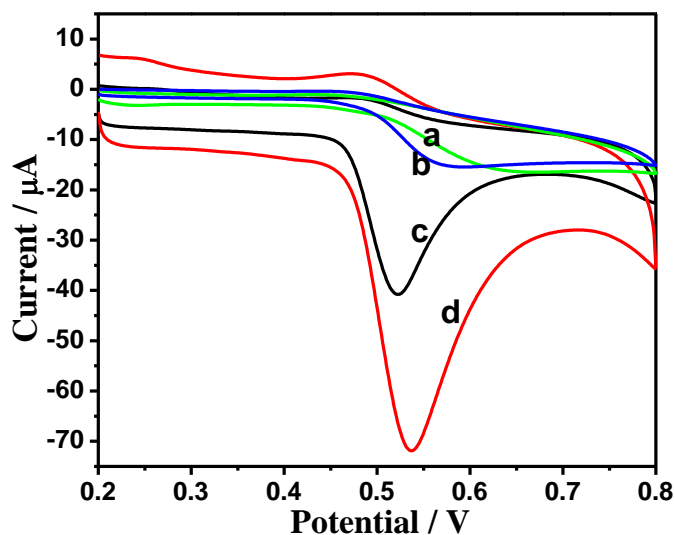


Figure 5. CVs of Au@Ag NPs/GCE (a), GCE (b), NG/GCE (c) and NG-Au@Ag NPs/GCE (d) in the 1.2 mM GA solution, 10 mL PBS ($\text{pH} = 2.0$), scan rate of 50 mV/s.

To investigate the interface features of modified electrodes, the voltammetric responses of Au@Ag NPs/GCE (a), GCE (b), NG/GCE (c) and NG-Au@Ag NPs/GCE (d) toward determination of GA with CV were compared and shown in Fig. 5. Obviously, on Au@Ag NPs/GCE (curve a) and GCE (curve b), the currents had changed little and were almost constant. However, it was cleared that rather high currents of GA were obtained on NG/GCE (curve c) and NG-Au@Ag NPs/GCE (curve d) due to the active sites present in NG. It was the NG-Au@Ag NPs/GCE that has the highest currents, implying that NG-Au@Ag NPs/GCE can determine GA with high sensitivity.

3.4.2 Influence of pH

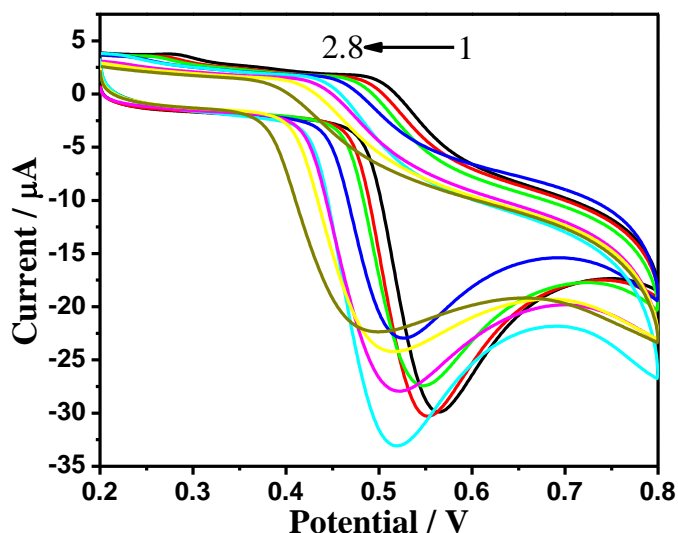


Figure 6. CVs of NG-Au@Ag NPs/GCE in PBS with different pH values (1, 1.2、1.4、1.8、2.0、2.2、2.4、2.8), 1.2 μM GA, scan rate of 50 mV/s.

The electrochemical responses of 1.2 mM GA on NG-Au@Ag NPs/GCE with different pH values ranging from 1.0 to 2.8 were investigated (Fig. 6). It was found that the peak currents (I_p) increased with the increasing of pH value until pH value reached to 2.0, and decreased slightly with the further increase of pH value. Therefore, pH 2.0 was selected as the suitable pH for determinate of GA in further experiments.

3.4.3 Effect of scan rate

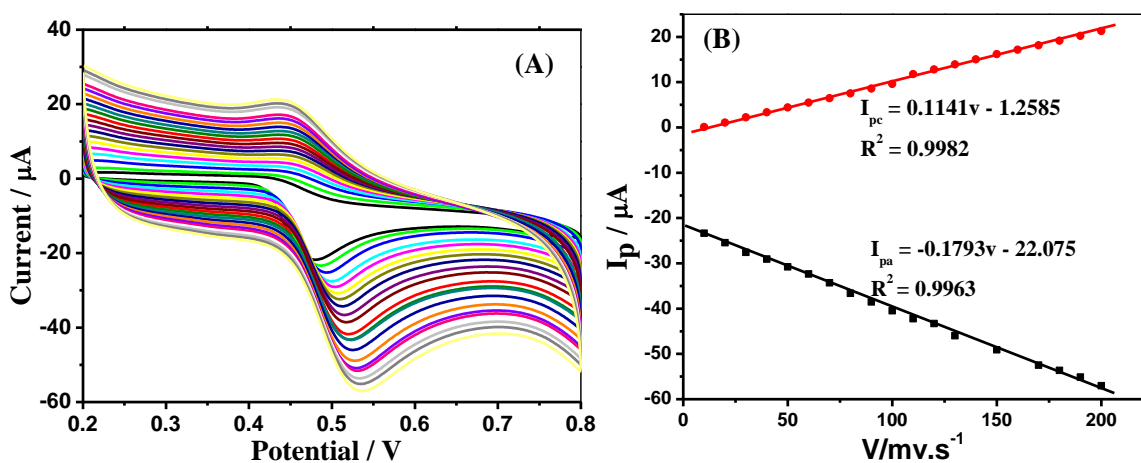


Figure 7. (A) CVs of NG-Au@Ag NPs/GCE. 1.2 mM GA, pH= 2.0, scan rate: 10, 20, 30, 40, 50, 60, 70, 80, 90, 100, 110, 120, 130, 140, 150, 160, 170, 180, 190, 200 mV/s). (B) Linear relationship of cathodic and anodic peak current versus vs. scan rate.

CVs of NG-Au@Ag NPs/GCE in 10 mL PBS (pH= 2.0) containing 1.2 mM GA were recorded and shown in Fig. 7. With the scan rate increasing from 10 to 200 mV/s, the I_p increased simultaneously and the peaks distance showed a remarkable enlargement (Fig. 7(A)). A good linear relationship existed between the anode (I_{pa}) and cathode (I_{pc}) peak currents under the scan rate range from 10 to 200 mV/s (Fig. 7(B)), meaning the surface-controlled process [13, 24].

3.4.4 Determination of GA on NG-Au@Ag NPs/GCE

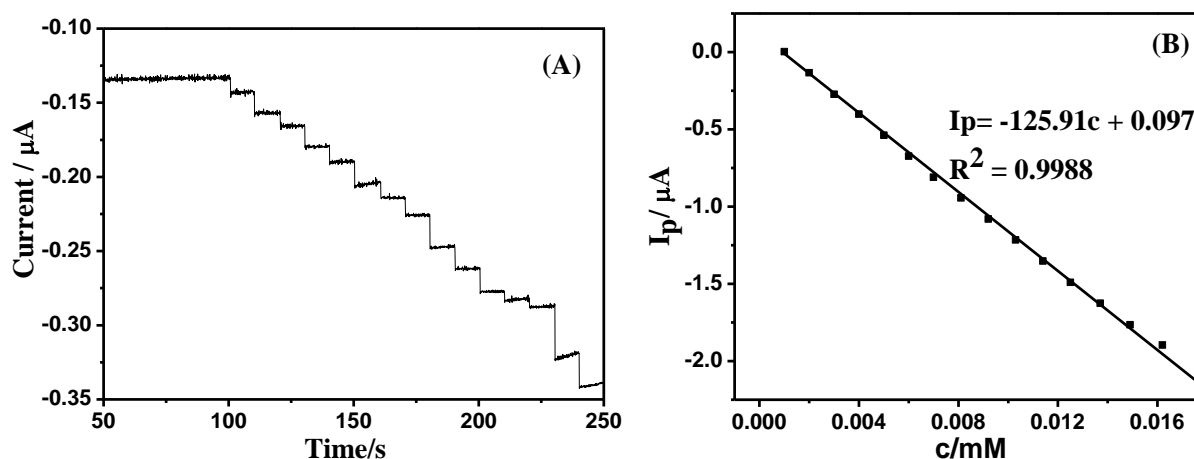


Figure 8. (A) Amperometric response at NG-Au@Ag NPs/GCE in 0.20 M PBS (pH= 2.0). GA concentrations: 1.0×10^{-6} - 1.62×10^{-5} M. (B) The relationship of I_p and GA concentration.

The amperometric *i-t* curve was investigated for determination of GA using NG-Au@Ag NPs/GCE in 0.2 M PBS (pH = 2.0) as shown in Fig. 8(A). A fast response was obtained for every addition of GA on NG-Au@Ag NPs/GCE. The I_p increased linearly with the increasing of the concentrations of GA (1.0×10^{-6} - 1.62×10^{-5} M). As shown in Fig. 8(B), the linear regression can be obtained as: $I_p = -125.91c$ (mM) + 0.097 ($R^2 = 0.9988$), and the calculated detection limits was 3.17×10^{-9} M (S/N=3). The comparison of similar electrodes and NG-Au@Ag NPs/GCE for GA determination was shown in Table 1.

Table 1. Comparison of similar electrodes and NG-Au@Ag NPs/GCE for GA determination

Electrodes	Linear range	Detection limit	Samples	Reference
SiO ₂ nanoparticle-CPE	8.0×10^{-7} - 1.0×10^{-4} M	2.5×10^{-7} M	Water, teas and juice	[1]
AuMCs/SF-GR/GCE	0.05-8 μ M	10.7 nM	Black tea and <i>Cortex moutan</i>	[3]
PEP/GCE	1.0-20 μ M	6.63×10^{-7} M	Black tea	[13]
ZrO ₂ -ChCl-AuNPs/CPE	0.22-55 μ M	25 nM	Human urine	[25]
NG-Au@Ag NPs/GCE	1.0×10^{-6} - 1.62×10^{-5} M	3.17×10^{-9} M	Black tea	This work

3.4.5 Stability of the Au@Ag NPs/GCE

The electrocatalytic characteristics of the NG-Au@Ag NPs toward the electrocatalysis of GA are moderately stable due to the invariable CVs curves after the NG-Au@Ag NPs/GCE was scanned continuously for 50 cycles at 50 mV/s (Fig. 9), indicating the excellent stability of NG-Au@Ag NPs/GCE. Furthermore, the results implied that the catalytic durability of NG-Au@Ag NPs was improved due to the bonding between Au@Ag NPs and NG.

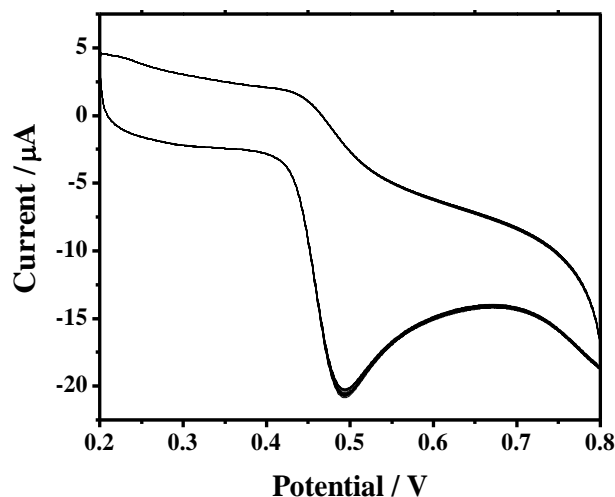


Figure 9. CVs of GA electrocatalytic reaction at the NG-Au@Ag NPs/GCE in 10 mL 0.20 M PBS (pH = 2.0) containing 1.2 mM GA for 50 consecutive cycles.

3.4.6 Sample analysis

Table 2. Results of GA detection in black tea samples (n=3).

Sample	Original (μM)	Added (μM)	Found (μM)	Recovery (%)	RSD (%)
1	0.98	20	21.03	100.25	2.03
2	0.95	25	24.98	96.12	1.74
3	0.101	30	30.28	100.50	1.52

In this study, black tea was selected as real sample for determination of GA by the proposed method to evaluate the feasibility and applicability. To prepare the solution for determination of GA, 0.05 g black teas were added into 50 mL of boiled water and heated for 10 min. And then, the solution was diluted to 100 mL with PBS (pH = 2.0) after filtering and the desired working solutions for GA detection was obtained. Under the optimal experimental procedure, the recovery range and RSD were 96.12-100.50% and 1.52-2.03% (Table 2), respectively, indicating that the proposed method was reasonable for GA determination.

4. CONCLUSIONS

In summary, a hydrothermal method for preparation of N-doped graphene (NG) with a high relative atomic ratio of nitrogen (7.34%) has been investigated. Then, Au@Ag core-shell nanoparticles (Au@Ag NPs) were facilely embedded in NG to prepare N-doped Au@Ag core-shell nanoparticles (NG-Au@Ag NPs). After that, the NG-Au@Ag NPs were dropped on glassy carbon electrode (GCE) to obtain a modified gold electrode (NG-Au@Ag NPs/GCE). Significantly, the electrochemical sensor for gallic acid (GA) determination showed an excellent response and exhibited a good linear range of 1.0×10^{-6} - 1.62×10^{-5} M with the detection limit of 3.17×10^{-9} M (S/N=3). The recovery range and relative standard deviation (RSD) were 96.12-100.50% and 1.52-2.03% for determination of GA in black teas, respectively.

ACKNOWLEDGMENTS

The authors gratefully acknowledge the financial support from the Yunnan education department of Scientific Research Foundation (2018JS478, 2019J1183), Yunnan Local Colleges Applied Basic Research Projects (2018FH001-114, 2018FH001-049 and 2017FD157) and the National Natural Science Foundation of China (51362012, 51662007 and 51574213)

References

1. J. Tashkhourian, S.F. Nami-Ana, *Mater. Sci. Eng. C*, 52 (2015) 103-110.
2. D.M. Stankovic, M. Ognjanovic, F. Martin, L. Svorc, J. Mariano, B. Antic, *Anal Biochem.*, 539 (2017) 104-112.
3. Z.X. Liang, H.Y. Zhai, Z.G. Chen, H.H. Wang, S.M. Wang, Q. Zhou, X.T. Huang, *Sensor. Actuat. B:Chem.*, 224 (2016) 915-925.
4. K. Narumi, J.I. Sonoda, K. Shiotani, M. Shigeru, M. Shibata, A. Kawachi, E. Tomishige, K. Sato, T. Motoya, *J. Chromatogr. B*, 945-946 (2014) 147-153.
5. R. Song, Y. Cheng, Y. Tian, Z.J. Zhang, *Chin. J. Nat. Medicine*, 10 (2012) 275-278.
6. Y.G. Zuo, H. Chen, Y.W. Deng, *Talanta*, 57 (2002) 307-316.
7. T. Dhanani, R. Singh, S. Kumar, *J. Food Drug Anal.*, 25 (2017) 691-698.
8. K.B. Wang, Q.C. Chen, Y. Lin, S.S. Yu, H.Y. Lin, J.N. Huang, Z.H. Liu, *J. Chromatogr. B*, 1017-1018 (2016) 221-225.
9. M. Bedner, D.L. Duewer, *Anal. Chem.*, 83 (2011) 6169-6176.
10. C. Xiong, Y. Wang, H. Qu, L.J. Zhang, L.Z. Qiu, W. Chen, F. Yan, L. Zheng, *Sensor. Actuat. B:Chem.*, 246 (2017) 235-242.
11. B.B. Petkovic, D. Stankovic, M. Milcic, S.P. Sovilj, D. Manojlovic, *Talanta*, 132 (2015) 513-519.
12. J.H. Luo, B.L. Li, N.B. Li, H.Q. Luo, *Sensor. Actuat. B:Chem.*, 186 (2013) 84-89.
13. R. Abdel-Hamid, E.F. Newair, *J. Electroanal. Chem.*, 704 (2013) 32-37.
14. G. Frens, *Nat. Phys. Sci.*, 241 (1973) 20-22.
15. W.S. Hummers, R.E. Offerman, *J. Am. Chem. Soc.*, 80 (1958) 1339.
16. N. Pandiyan, B. Murugesan, M. Arumugam, J. Sonamuthu, S. Samayanan, S. Mahalingam, *J. Photochem. Photobiol. B*, 198 (2019) 111559.
17. R. Pérez-Hernández, C. Gutiérrez-Wing, G. Mondragón-Galicia, A. Gutiérrez-Martínez, F.L. Deepak, D. Mendoza-Anaya, *Catal.Today*, 212 (2013) 225-231.
18. Y.W. Chen, W.G. Wang, S.H. Zhou, *Mater. Lett.*, 65 (2011) 2649-2651.
19. S.N. Wang, S. Liu, J.Y. Zhang, Y. Cao, *Talanta*, 198 (2019) 501-509.
20. X.L. Chen, G.W. Zhang, L. Shi, S.Q. Pan, W. Liu, H.B. Pan, *Mater. Sci. Eng. C*, 65 (2016) 80-89.
21. X.L. Chen, G.M. Yang, S.P. Feng, L. Shi, Z.L. Huang, H.B. Pan, W. Liu, *Appl. Surf. Sci.*, 402 (2017)

232-244.

22. X.Q. Li, L.S. Wang, Q. Wu, Z.C. Chen, X.F. Lin, *J. Electroanal. Chem.*, 735 (2014) 19-23.

23. F.Y. Kong, L. Yao, R.F. Li, H.Y. Li, Z.X. Wang, W.X. Lv, W. Wang, *J. Alloy. Compd.*, 797 (2019) 413-420.

24. Y.L. Su, S.H. Cheng, *Anal. Chim. Acta*, 901 (2015) 41-50.

25. S.A. Shahmirifard, M. Ghaedi, Z. Razmi, S. Hajati, *Biosens. Bioelectron.*, 114 (2018) 30-36.

© 2020 The Authors. Published by ESG (www.electrochemsci.org). This article is an open access article distributed under the terms and conditions of the Creative Commons Attribution license (<http://creativecommons.org/licenses/by/4.0/>).